Article

Characterization of a Modified Clinical Linear Accelerator for Ultra-High Dose Rate Beam Delivery

Umberto Deut [1,2,*,†], Aurora Camperi [2,†], Cristiano Cavicchi [3], Roberto Cirio [1,2], Emanuele Maria Data [1,2], Elisabetta Alessandra Durisi [1,2], Veronica Ferrero [1,2], Arianna Ferro [1,2], Simona Giordanengo [2], Oscar Martì Villarreal [4], Felix Mas Milian [1,2,5], Elisabetta Medina [1,2], Diango M. Montalvan Olivares [1,2], Franco Mostardi [1,2], Valeria Monti [1,2], Roberto Sacchi [1,2], Edoardo Salmeri [3] and Anna Vignati [1,2,‡]

1   Department of Physics, University of Turin, 10125 Turin, Italy; anna.vignati@unito.it (A.V.)
2   Section of Turin, National Institute of Nuclear Physics (INFN), 10125 Turin, Italy
3   Elekta S.p.A., 20864 Agrate Brianza, Italy
4   Center for Sensors and Devices, Bruno Kessler Foundation (FBK), 38122 Trento, Italy
5   Department of Exact and Technological Sciences, Universidade Estadual de Santa Cruz, Ilhéus 45662-900, Brazil
*   Correspondence: umberto.deut@unito.it
†   These authors contributed equally to this work and share first authorship.
‡   Last author.

Abstract: Irradiations at Ultra-High Dose Rate (UHDR) regimes, exceeding 40 Gy/s in single fractions lasting less than 200 ms, have shown an equivalent antitumor effect compared to conventional radiotherapy with reduced harm to normal tissues. This work details the hardware and software modifications implemented to deliver 10 MeV UHDR electron beams with a linear accelerator Elekta SL 18 MV and the beam characteristics obtained. GafChromic EBT XD films and an Advanced Markus chamber were used for dosimetry characterization, while a silicon sensor assessed the machine's beam pulses stability and repeatability. The dose per pulse, average dose rate and instantaneous dose rate in the pulse were evaluated for four experimental settings, varying the source-to-surface distance and the beam collimation, i.e., with and without the use of a cylindrical applicator. The results showed a dose per pulse from 0.6 Gy to a few tens of Gy and an average dose rate up to 300 Gy/s. The obtained results demonstrate the possibility to perform in vitro radiobiology experiments and test new technologies for beam monitoring and dosimetry at the upgraded LINAC, thus contributing to the electron UHDR research field.

Keywords: ultra-high dose rate; FLASH radiotherapy; LINAC; dosimetry; electron beam; silicon sensors; GafChromic films

1. Introduction

Research on Ultra-High Dose Rate Radiotherapy (UHDR RT) is experiencing significant growth, prompting the scientific community to investigate the reasons behind the normal tissue sparing effect, known as the FLASH effect. The FLASH effect refers to the phenomenon where a high dose is delivered in a very short time, resulting in less damage to normal tissues compared to conventional dose rates while maintaining the same tumor control. The challenges associated include understanding the underlying radiobiological mechanisms, the generation of high-quality beams, ensuring accurate dosimetry and closely monitoring the radiation beam during treatment [1–7].

Although the beam characteristics that induce the FLASH effect are not yet understood, there is a consensus on the relevance of certain irradiation parameters' thresholds. UHDR RT requires instantaneous dose rates around 10^5 Gy/s and at least 40 Gy/s as average dose rates [1,2], with single irradiation fractions lasting less than 200 ms [7].

The availability of machines capable of delivering UHDR beams is crucial for every aspect of the research and to take the necessary steps toward potential clinical applications, from radiobiological studies [2,8] to the development of dedicated Treatment Planning Systems (TPS) [8,9]. For these reasons, this work addresses the need for UHDR RT research facilities focusing on the growing interest in modifying clinical linear accelerators (LINACs), a method that gathered successful results over the last decade [10–14].

This work presents the reversible modification of a LINAC Elekta SL 18 MV toward the delivery of a 10 MeV electron UHDR beam and its dosimetry characteristics in different irradiation settings, i.e., varying the source-to-surface distance (SSD) and with the optional use of a cylindrical polymethyl methacrylate (PMMA) applicator.

Dosimetry measurements in UHDR mode were performed with GafChromic films EBT XD and compared to the results obtained for the conventional regime with both films and an Advanced Markus (AM) ionization chamber. Thin silicon sensors, placed at the exit of the accelerator head, were used to monitor the output beam pulses and evaluate their temporal uniformity within the pulse, as well as the pulse-by-pulse stability.

This upgrade of the LINAC Elekta SL 18 MV facility provides the researchers a valuable tool for UHDR studies, allowing the testing of different beam monitoring technologies and perform radiobiological experiments. Additionally, the positioning of perforated templates at the applicator's end could allow future studies on the characteristics of Spatially Fractionated Radiation Therapy (SFRT) [15,16].

2. Materials and Methods

The LINAC Elekta SL 18 MV was installed in 2016 at the Physics Department of the University of Turin (UNITO) and is entirely dedicated to research. This machine can generate both X-rays (up to 18 MV) and electrons (4–18 MeV), delivering the beam in 2 µs pulses at a Pulse Repetition Frequency (PRF) between 6 and 400 Hz. The accelerator head is equipped with multi-leaf collimators (MLC) and diaphragms that precisely shape the beam, allowing radiation fields up to 40×40 cm^2 at the isocenter position. It also contains a monitoring system consisting of two independent ionization chambers (ICs), one acting as the primary reference and the second as a backup.

The 10 MeV electron beam can be delivered both in the standard LINAC clinical configuration (conventional mode) and with the high dose rate LINAC upgrade described in Section 2.1 (UHDR mode).

The beam pulse characterization with a silicon sensor and dose measurements, respectively, described in Sections 2.2 and 2.3, were performed for four irradiation settings, each one featuring different SSDs and collimation of the beam (Figure 1):

(i)   At the isocenter position (SSD = 100 cm);
(ii)   At the isocenter position with a PMMA cylindrical applicator with a 5 cm inner diameter;
(iii)   At the crosshair foil (SSD = 52.9 cm) at the exit of the LINAC head;
(iv)   In the wedge tray (SSD = 18.6 cm) inside the LINAC head.

For all the settings, the irradiation field size was fixed at 10×10 cm^2 at the isocenter position (i), resulting in smaller field sizes for the configurations closer to the source.

The crosshair foil position (iii) is the closest point to the source where standard dosimetry procedures can still be applied, while the wedge tray position (iv) can only be evaluated with in-air measurements.
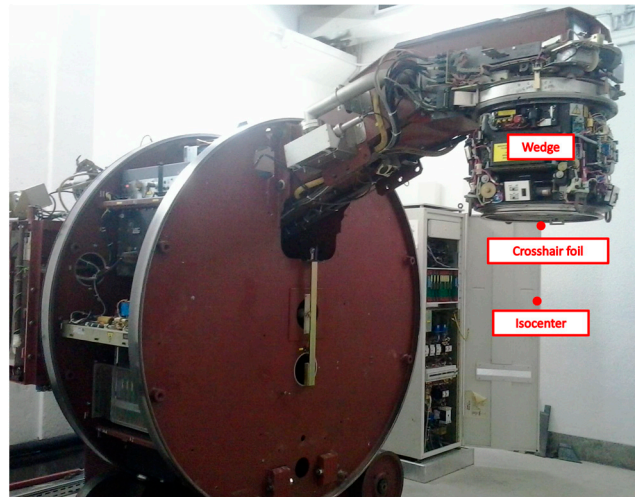
Figure 1. The LINAC Elekta SL 18 MV with three (out of the four) irradiation settings available: isocenter (i), crosshair foil (iii) and wedge (iv).

2.1. Clinical Accelerator Upgrade

The upgrade of the LINAC aiming to generate a UHDR electron beam was supervised by Elekta technicians, who implemented both hardware and software modifications to the machine, following the work of Lempart et al. [10].

In the control console, the default parameters of the 10 MV photon mode were adjusted to deliver an electron beam, preventing the X-ray target from interfering with the beam path. All the filters, including the wedge and the shutter foil, were removed, leaving a free spot of approximately 100 cm^3 on the wedge tray between the ICs and the light mirror. This spot corresponds to the irradiation setting iv, listed above.

The electron gun filament current increased from the conventional 5.6 A to 7.3 A. The bending magnet intensity was tuned to optimize the beam transport and maximize the accelerated beam current under the new conditions. The power drawn from the magnetron was increased to approximately 6 kW, which remained below the specified maximum power of 7 kW. The gun current and magnetron settings were changed from the control panel using LINAC's proprietary software and following the instructions of the company's technicians. Throughout the process, the magnetron's power was monitored using an oscilloscope connected to one of the accelerator's test points. As the gun current was increased, the voltage and magnetron current were controlled, always trying to stay within the safety range of the datasheet specifications.

Each time the LINAC is started, a standard warm-up procedure is performed by delivering about 1000 Monitor Units (MU) of a 15 MV X-ray beam and about 1000 MU of the 10 MeV electron clinical beam to reach the optimal working conditions. Once the regime is switched to UHDR mode, the parameters related to the electron gun current, gun aim, gun standby and tuner control are manually adjusted to the optimal values. The parameters generally experience small variations during the optimization, and the operation usually requires a few beam deliveries for prior adjustments. During LINAC operation, the water temperature is maintained between 26 °C and 28 °C, a range in which the best performance can be achieved.

Specific interlocks must be overridden to operate the LINAC in UHDR conditions [10,11,13]. To prevent the internal ICs interlock from being triggered, a custom attenuator circuit provided by Elekta was connected to the LINAC, as similarly documented by Snyder et al. [11], who obtained comparable UHDR dose rates to those found in this study. This circuit was installed between the ICs and the dosimetry system of the accelerator to reduce the current signal from the ICs, thus avoiding the activation of the interlocks.

The attenuator circuit makes the ICs' readings unreliable, and so they cannot be used to monitor the dose delivered. Therefore, a pulse counter circuit (PCC) was developed to control the LINAC delivery in UHDR mode by counting the number of beam pulses [10,12].

The circuit converts the current signal generated in an unbiased silicon diode sensor into voltage signals using a transimpedance amplifier. The voltage signals are then filtered through a Sallen–Key filter and amplified to produce an acceptable input signal for a Schmitt Trigger. The resulting 5 V amplitude square pulses are counted using an Arduino NANO board. The PCC accuracy was tested with the pulsed beam of the LINAC by checking the match between the PCC output and the number of oscilloscope readings, and under these circumstances, no pulse loss was observed. All measurements reported in this study are referred to the High Power (HP) mode of the RF injection cycle of the magnetron, where two charging cycles occur before the thyratron is triggered by the Pulse-Forming Network (PFN). HP mode is needed for reaching the highest possible dose rates. However, a Low Power (LP) mode is also available, resulting in dose rate values intermediate between the conventional rate and UHDR. The availability of three LINAC modalities (conventional, UHDR LP and UHDR HP) can be exploited to vary the delivered dose while maintaining the same experimental setup.

All the reported modifications do not compromise the operation of the LINAC in the conventional mode, and few minutes are required to switch between the irradiation modalities.

2.2. Pulse Characterization with Silicon Sensors

The temporal structure and the consistency of the output pulses after the LINAC modification were measured with a silicon sensor previously tested for response linearity up to doses of 10 Gy/pulse at the SIT ElectronFlash accelerator (9 MeV UHDR electron beam) at Centro Pisano FLASH Radiotherapy (CPFR, Pisa) [17]. The sensor was manufactured by the Fondazione Bruno Kessler (FBK) and consists of an epitaxial substrate grown on a low-resistivity silicon layer. This device is a square with a 4.5 mm edge, an active thickness of 45 μm and a support layer of 570 μm. It is segmented in eight pads with different active areas (0.03 mm^2–2.3 mm^2) isolated by guard rings. For the measurements, the device was mounted on a high voltage (HV) distribution PCB (Figure 2a) designed to polarize the sensor from the back via a copper layer with a window behind the sensor so that only a 2 mm thick layer of FR4 resin is behind the sensor. Bonding wires (Al 1% Si) with a diameter of 25 μm, allowing a maximum rated current of 500 mA, were used to connect the 2 mm^2 pad to an output channel of the board and to ground the guard ring.

(**a**)   (**b**)
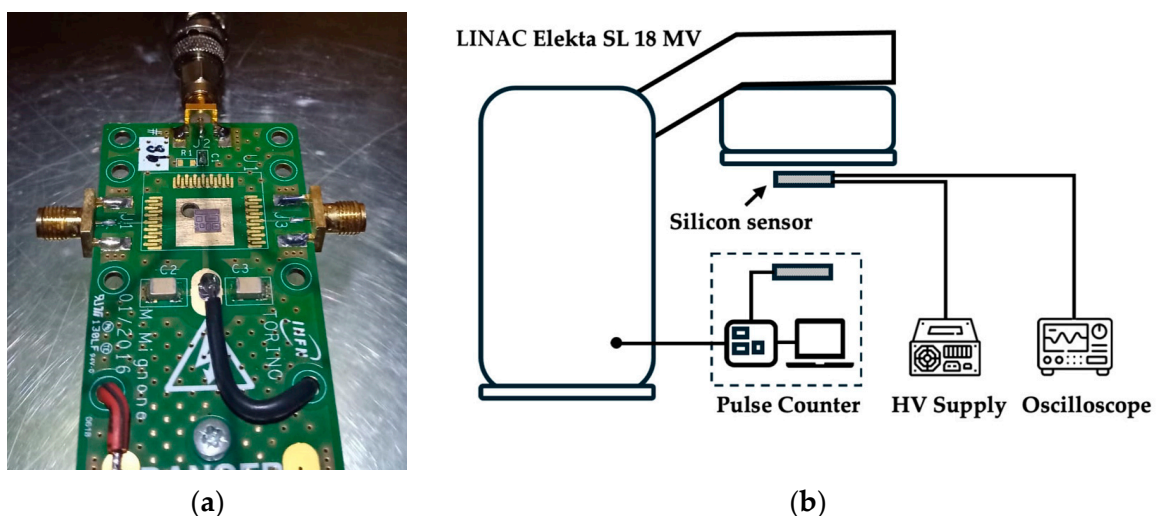
Figure 2. (**a**) PCB with a bonded sensor in the center. (**b**) Schematic of the setup with the silicon sensor at the crosshair foil position (iii).

The multipad sensor was reverse biased at -200 V and the stability of the HV supply was monitored during the acquisitions to guarantee the stability of the applied voltage. The sensor was manually positioned at the center of the field at the crosshair foil position (iii) with an uncertainty of 5 mm in the transverse plane.

The output channel was connected via a coaxial cable to a Keysight Infiniium S-Series oscilloscope (2.5 GHz, 20 GSa/s, Model: DSOS254A) to read and store the output pulse signals delivered by the LINAC (Figure 2b). The produced charge per pulse was determined by dividing the signal area by the input impedance of the oscilloscope (50 Ω). Signal processing involved only the voltage offset removal from the signal calculated as the average of the first 10,000 off-pulse samples in each collected waveform.

The stability and reproducibility of the delivered pulses were then studied with repeated measurements of the charge per pulse generated under consecutive pulses and on different days.

2.3. Dosimetry Measurements

The beam energy verification after the upgrade was performed by measuring the percentage depth dose (PDD) curves in both conventional and UHDR modes. In the first case, a complete PDD curve was obtained using the Advanced Markus (AM) chamber (Type 34045, PTW, Freiburg, Germany) and a 1D scanner water tank (Sun Nuclear Corporation, Melbourne, FL, USA) (Figure 3a), following the TRS-398 guidelines of the International Atomic Energy Agency (IAEA) [18].

(a)   **(b)**
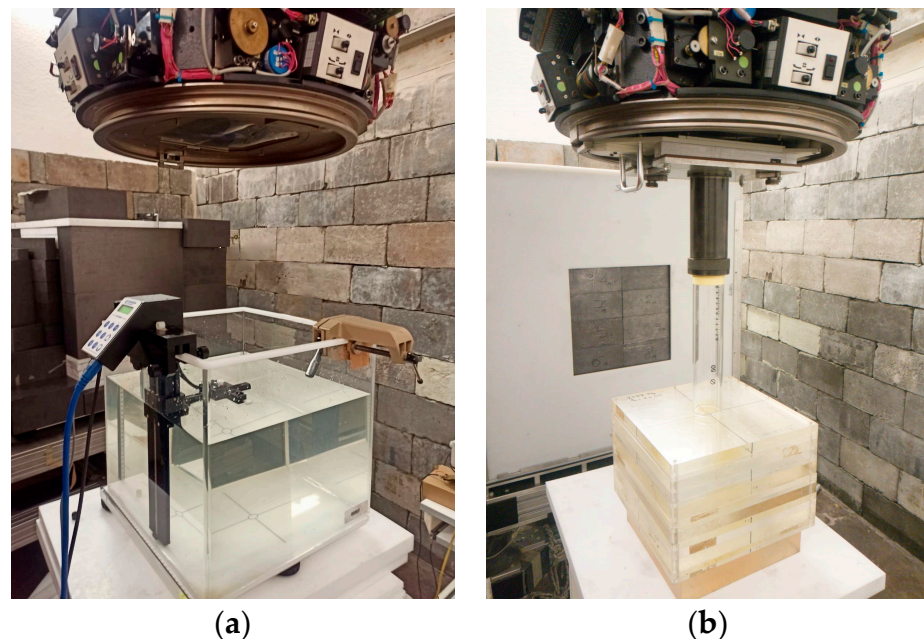
Figure 3. (**a**) One-dimensional water phantom positioned at the isocenter (i); (**b**) setup with the applicator (ii) and the PMMA phantom.

In the case of UHDR irradiations, PDD curves were collected by placing EBT XD GafChromic films (Ashland, Bridgewater, MA, USA) between PMMA slabs to avoid distortions due to the large charge recombination observed in ICs at large dose rates [19,20].

PDD curves were measured with the water phantom and the PMMA slabs at the isocenter position both with and without the applicator (irradiation settings *ii* and *i*, respectively). A holder secured the applicator at the crosshair foil position, with its exit side aligned with the surface of the water tank or the PMMA (Figure 3b). The detector was always placed transversely at the center of the field.

From these curves, it was possible to calculate dosimetry parameters such as the practical range (R_P) and the depths where the absorbed dose was 50% (R_{50}) and 80%

(R_{80}) of the maximum. Based on R_{50}, the reference depth (z_{ref}), the position at which the evaluation of the absorbed dose should be performed, was calculated as recommended in [18] as follows:

$$z_{ref} = 0.6R_{50} - 0.1 \tag{1}$$

EBT XD GafChromic films were used to quantify the beam output in terms of total dose, average dose per pulse (DPP), instantaneous dose rate in the pulse and the average dose rate. The instantaneous dose rate in the pulse was obtained from the average DPP divided by the pulse duration τ (2 μs), while the average dose rate was calculated from the number of delivered pulses (N) at a fixed PRF of 100 Hz, as reported by Cetnar et al. [13].

$$Average\ Dose\ Rate = \frac{total\ dose}{\frac{N-1}{PRF} + \tau} \tag{2}$$

For these measurements, EBT XD films were placed in the PMMA phantom with a buildup thickness of 18 mm. This thickness was selected based on the z_{ref} values determined from the PDD analysis and considering the correction factors for transforming the water thickness into the equivalent PMMA thickness. In the wedge tray position, due to space restrictions, the films were irradiated without buildup.

Furthermore, GafChromic films were also used to evaluate the beam spatial profiles in both irradiation modalities. When using the films, the total number of pulses N was changed according to the setting to avoid film saturation.

The absolute dose of the irradiated films was evaluated in terms of net optical density (OD), as established in the manufacturer's guidelines and protocols [21,22]. For this purpose, the films were scanned with a flatbed color scanner (Model: Epson Expression 12000XL) used in transmission mode, acquiring 48-bit RGB images with a resolution of 100 dpi. The films were scanned twice: before the irradiation to save the background image and 24 h after irradiation to determine the absorbed dose. The analysis of the images was executed with a program developed in Matlab, where the net OD was calculated from the pixel-by-pixel difference between the OD of the irradiated and the background images. The net ODs were calculated over a Region of Interest (ROI) of the same size to the active area of the AM chamber (0.20 cm^2). The conversion from the net OD to dose was executed with two different calibration curves: the first one relying on the 10 MeV conventional electron beam in the 0.5–10 Gy range, and the second one on the 9 MeV UHDR electron beam delivered at the CPFR (Pisa, Italy) for the range of 0.5–40 Gy. Below the 10 Gy threshold, the observed difference between the calibration curves was less than 5%, which corresponds to the standard uncertainty associated with the dose obtained with a GafChromic film [13]. For doses higher than 10 Gy, only the calibration relying on the CPFR irradiations was used. For further reliability, a calibration curve was also determined by scanning the films one week after irradiation. The difference between the curves referring to 24 h and one week is 2.5% (Figure 4).

All the calibration curves were fitted with the following rational function:

$$netOD = a + \frac{b}{Dose - c} \tag{3}$$

where a, b and c are free parameters.

Finally, a study of the output factor (OF) was conducted in both irradiation modalities at the isocenter position (i), varying the beam field from 3×3 cm^2 to 30×30 cm^2.
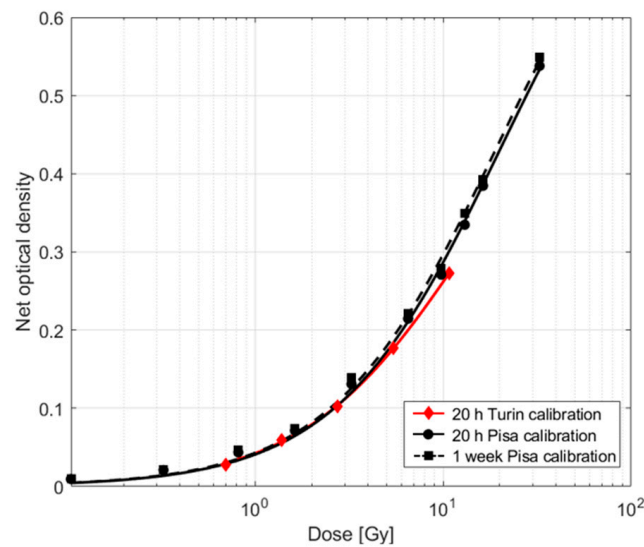
Figure 4. Different EBT XD calibrations with best fit curves.

3. Results

3.1. Beam Pulse Characterization

The monitoring of the beam with the silicon sensor allows a qualitative and quantitative analysis of the beam pulses. A comparison of the voltage pulses acquired with the oscilloscope at the different irradiation setting positions is shown in Figure 5.
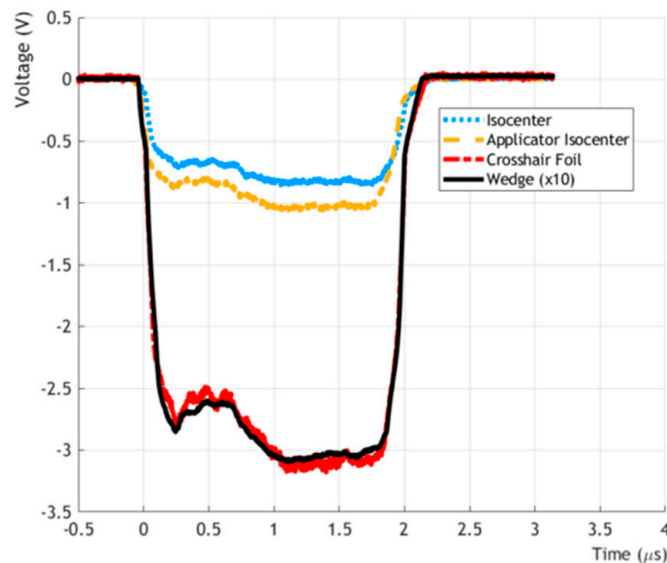

Figure 5. Output voltage pulse generated by the 10 MeV UDHR electron beam from the LINAC on a silicon sensor (60 um thickness) recorded by the oscilloscope with the different irradiation settings. The wedge signal was divided by a factor of 10 for ease of comparison.

The figure demonstrates the capability of increasing, through the optimization procedure, the charge per pulse while maintaining the 2 µs pulse shape and duration mostly unchanged. The boxplots in Figure 6 show the analysis of the charge collected per pulse in the UHDR mode at the crosshair foil for qualifying the performance of the accelerator; the median value has been presented as reference, while the range and 25th and 75th percentiles provide information on the variability of the measure.
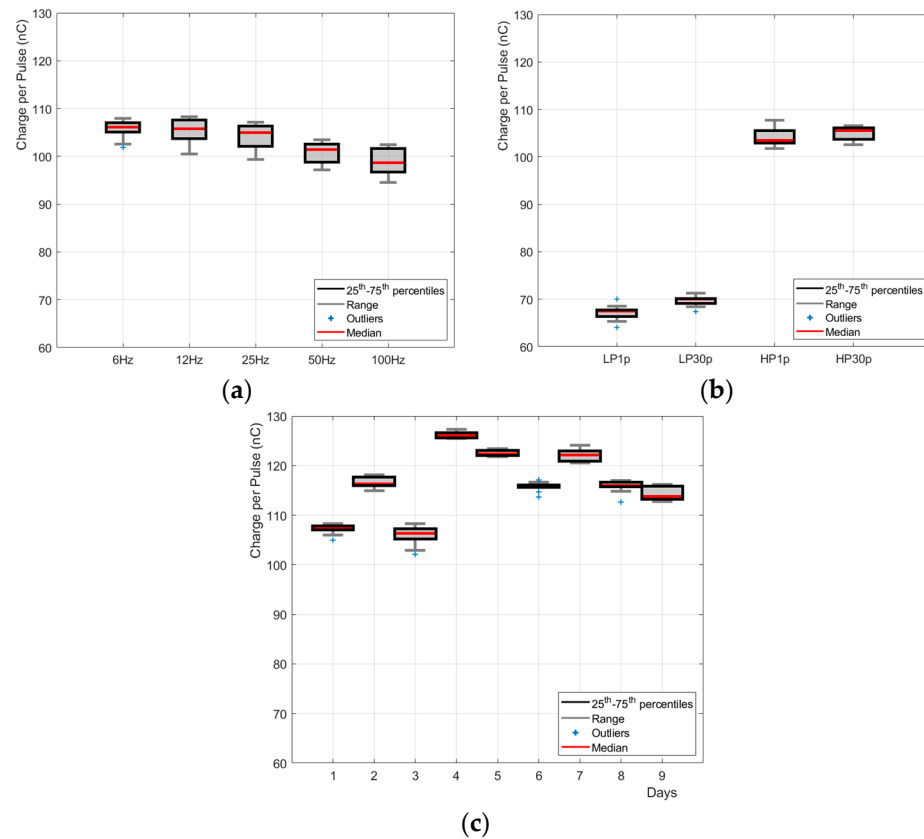
Figure 6. (**a**) Collected charge per pulse at the crosshair foil position for different PRFs. Each boxplot represents a total of 20 pulses delivered in HP mode. (**b**) Comparison of the charge per pulse at the crosshair foil position in LP and HP modes considering single pulse irradiations repeated 10 times (LP1p and HP1p) and 30 consecutive pulses (LP30p and HP30p. (**c**) Repeatability of the charge per pulse at the crosshair foil position acquired on different days in HP mode.

In Figure 6a, the collected charge per pulse at the crosshair foil position irradiating 20 consecutive pulses is presented as a function of the PRF. A 7% decrease in the median charge value is observed between the lowest and highest PRFs, while, at the same PRF, the maximum pulse-by-pulse deviation from the median value is 5%. The dose per pulse in ten single-pulse deliveries and in a delivery with 30 consecutive pulses are compared in Figure 6b for the two RF injection cycle modes (LP and HP), showing a maximum difference of the 3.7%. The LP mode exhibits a better pulse-by-pulse stability at the expense of a lower charge per pulse, which appears to be 35% lower compared to the HP mode. Indeed, consecutive beam deliveries in LP mode result in a variation of the charge of 2%, while in HP mode, the maximum deviation from the median is 3.8%. The reproducibility of the pulses in HP mode is presented in Figure 6c, where the charge per pulse at the crosshair measured in identical irradiations of 30 pulses with a PRF of 100 Hz was repeated on nine different days within three months. The deviation from the median value is less than 8% for 90% of the measurements performed.

3.2. Dosimetry

The UHDR PDD curves obtained with GafChromic films show good agreement with the curves obtained with both the AM chamber and films for the conventional 10 MeV electron beam (Figure 7). The maximum difference between R_{50} values is 3.6% and only the initial points (near to the surface) show an underdose that could be caused by some air gaps between the PMMA slabs or by the proximity to the film cut [23]. The dosimetry parameters mentioned in Section 2.3 were calculated and are shown in Table 1.

(**a**)　　　　　　　　　　　　　　(**b**)
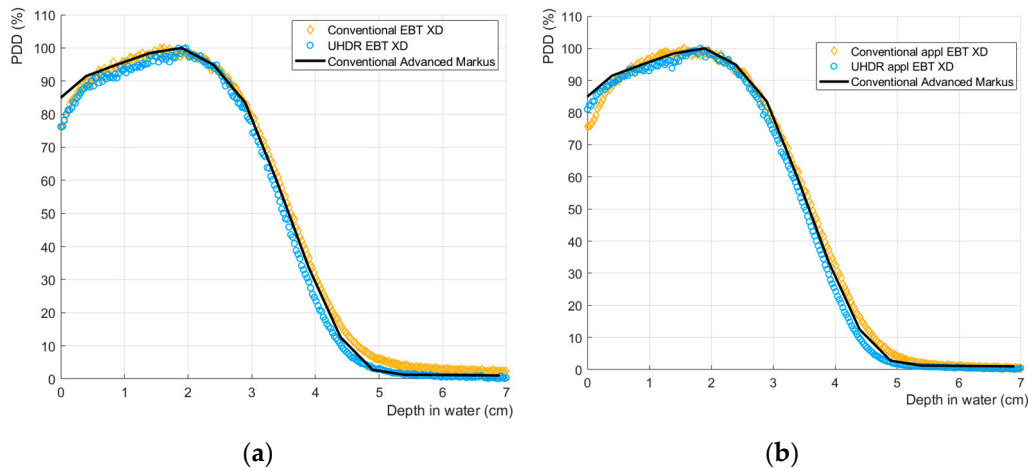
Figure 7. Comparison between PDD curves measured with the Advanced Markus and GafChromic films EBT XD in conventional and UHDR regimes (**a**) without the applicator and (**b**) with the applicator.

Table 1. Comparison of range parameters in water in conventional and UHDR modes.

Mode	Setup	R_{80} (cm)	R_{50} (cm)	R_p (cm)	z_{ref} (cm)
Conventional	Advanced Markus	2.95 ± 0.10	3.61 ± 0.11	4.75 ± 0.18	2.07 ± 0.07
	EBT XD	2.94 ± 0.07	3.65 ± 0.05	4.69 ± 0.26	2.09 ± 0.03
	EBT XD with the applicator	2.97 ± 0.05	3.67 ± 0.02	4.72 ± 0.24	2.10 ± 0.01
UHDR	EBT XD	2.88 ± 0.10	3.54 ± 0.10	4.55 ± 0.28	2.03 ± 0.06
	EBT XD with the applicator	2.89 ± 0.04	3.54 ± 0.02	4.55 ± 0.19	2.03 ± 0.01

The dosimetry values estimated with different detectors are comparable to each other and confirm that the modification of the LINAC did not affect the energy distribution of the beam, even when the applicator was inserted. The uncertainties of the R_{80} and R_{50} values are at most 3%, while the R_p values are characterized by larger uncertainties of 5% since they are calculated as the intersection between two interpolation lines. The R_{50} values reported in Table 1 are 7% smaller than the expected value for 10 MeV electrons [24], indicating that the most probable beam energy is slightly less than 10 MeV.

From the absorbed dose, measured for the four irradiation settings at the reference depth z_{ref}, it was possible to extract the DPP, the average dose rate (Equation (2)) and the instantaneous dose rate in the pulse. Results are reported in Table 2.

Table 2. Dosimetry results.

		Dose Per Pulse (Gy)		Average Dose Rate (Gy/s)		Instantaneous Dose Rate (Gy/s)	
	Mode	Conv	UHDR	Conv	UHDR	conv	UHDR
Setting	Isocenter	$(1.60 \pm 0.08) \times 10^{-4}$	0.63 ± 0.04	$(1.60 \pm 0.08) \times 10^{-2}$	83.6 ± 4.2	$(7.99 \pm 0.40) \times 10^1$	$(3.60 \pm 0.18) \times 10^5$
	Applicator	$(2.52 \pm 0.13) \times 10^{-4}$	0.81 ± 0.04	$(2.52 \pm 0.13) \times 10^{-2}$	89.5 ± 4.5	$(1.26 \pm 0.06) \times 10^2$	$(4.03 \pm 0.20) \times 10^5$
	Crosshair foil	$(6.76 \pm 0.34) \times 10^{-4}$	2.22 ± 0.11	$(6.76 \pm 0.34) \times 10^{-2}$	309 ± 16	$(3.38 \pm 0.17) \times 10^2$	$(12.3 \pm 0.6) \times 10^5$
	Wedge *	$(0.92 \pm 0.05) \times 10^{-2}$	27.2 ± 1.4	$(92.3 \pm 4.6) \times 10^{-2}$	n.d. **	$(4.61 \pm 0.23) \times 10^3$	$(136 \pm 7) \times 10^5$

* Dose in air without build up. ** n.d.: not determined.

As expected from previous studies [25], the comparison between conventional and UHDR modalities indicates an increase of the three dose quantities of at least three orders of magnitude for all the irradiation settings. At the wedge tray position (*iv*) in the UHDR regime, only one pulse was delivered to avoid exceeding the dose range of EBT XD films (40 Gy); thus, it was not possible to calculate the average dose rate for multiple pulses as in the other settings.

The use of the PMMA applicator results in an increase in the DPP at the isocenter of 57% and 28% in conventional and UHDR modes, respectively.

The beam profiles obtained from the scanned images are shown in Figure 8.
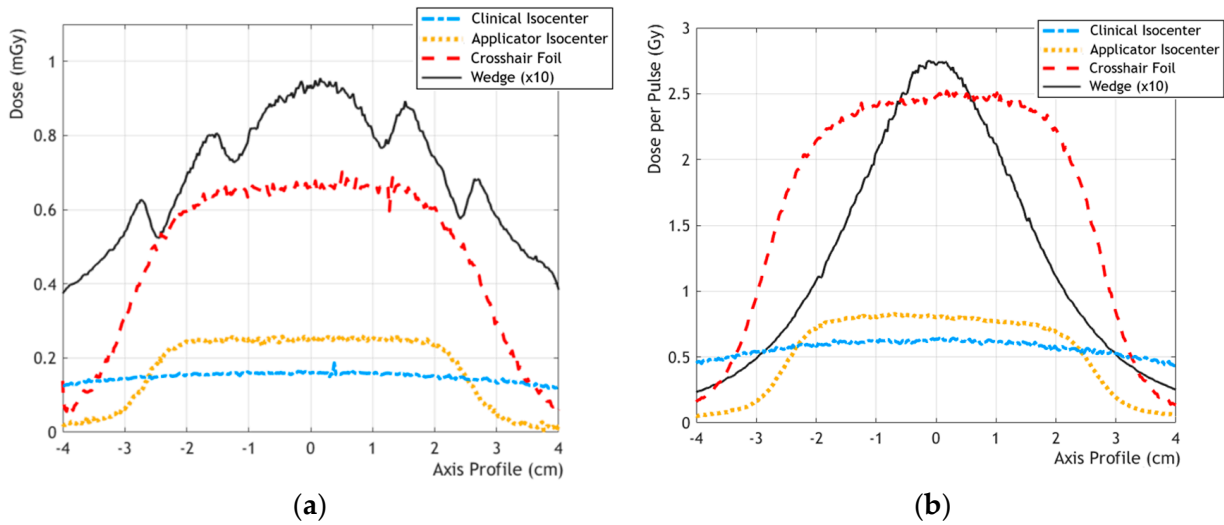
Figure 8. Dose profiles obtained from GafChromic films for the conventional (**a**) and UHDR modes (**b**). In both figures, the dose profiles at the wedge tray (setting *iv*) were divided by a factor of 10 for ease of comparison.

In the conventional mode, it is possible to note few bumps for the wedge setting profile. This can be attributed mainly to the geometry of the primary filters and of the secondary scattering foils, which have two sloped sections corresponding to specific scattering angles [10].

The study of the output factor in both irradiation modes is reported in Figure 9. In the conventional mode, there is good agreement between the AM chamber and the GafChromic films. The analysis of the UHDR mode data show a similar trend with the conventional mode data. For fields larger than 10×10 cm^2, UHDR values are systematically smaller, as reported by Dal Bello et al. [12], but all the differences are inside the error bars.
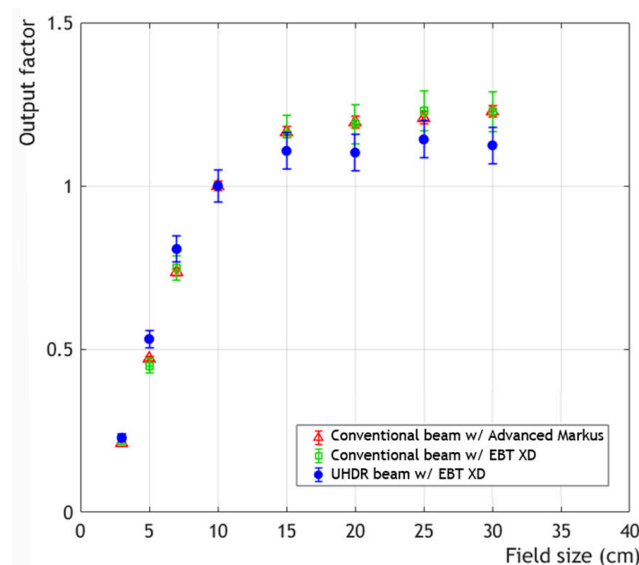
Figure 9. Output factor measured with the Advanced Markus and GafChromic films EBT XD in conventional and UHDR modes for different square field sizes.

4. Discussion

In this study, a LINAC Elekta SL 18 MV was upgraded to deliver a 10 MeV electron beam under UHDR conditions, and a characterization of the beam was performed. The main modifications consisted of removing the primary and secondary scattering foils, increasing the gun current and magnetron power and adjusting some parameters related to beam transport. Moreover, a custom PCC was developed to count the pulses delivered by the LINAC and stop the irradiation after the requested number of pulses, due to the unreliability of the IC chamber after the addition of an attenuator.

A silicon diode sensor, whose response has already been proven to be linear with the DPP [17], was used to verify the stability of the pulses within the same beam delivery and their repeatability across different beam deliveries and days. A variation of 3.7% in the charge per pulse was measured between single and consecutive pulse deliveries. Different irradiations within the same day showed good reproducibility with a maximum charge variation from the median of 2% for the LP mode and 4% for the HP mode. It is important to note that the verification of the UHDR pulse stability of the LINAC was performed when considering all pulses, including the first one, which, as shown, can be up to 4% smaller than the stable pulses. For this reason, the percentage variation shown in this study was slightly higher than that of Konradsson et al. [26], who modified a similar Elekta LINAC and reported deviations of less than 3% when the first pulse was excluded from the analysis. Since it is known that standby periods may impact the performance of the LINAC [26], the reproducibility was assessed on different days over a period of three months. The deviation of the charge per pulse measured by the silicon diode was less than 8% from the median value and is deemed acceptable for in vitro radiobiology studies.

The beam energy distribution was not affected by the LINAC modifications, as demonstrated by the PDD curves and the related parameters. The DPPs and the dose rates achieved in this study are comparable to those obtained for other modified LINACs [10–12], providing from a minimum 0.6 Gy/pulse ($3.6 \cdot 10^5$ Gy/s instantaneous dose rate) at the isocenter position (i) to a maximum 27 Gy/pulse ($136 \cdot 10^5$ Gy/s instantaneous dose rate) at the wedge tray position (iv). Average dose rate values over 300 Gy/s were reached at the crosshair foil position (iii) with a PRF of 100 Hz. These values allow planning both radiobiology experiments and test of instrumentation for the comparison of conventional and UHDR regimes, although the limited space available in the wedge irradiation setting needs to be carefully considered to design proper arrangements.

Several improvements of the reached performances will be investigated in the next months. The results reported in this study are referred to a PRF of 100 Hz and to LINAC software and hardware modifications corresponding to a maximum of 6 kW power drawn from the magnetron. Considering that the maximum PRF reachable for this LINAC is 400 Hz and that the magnetron power could be increased to 7 kW, further optimization of the delivery parameters will be studied, aiming at reaching higher DPP and average dose rates. Moreover, a correlation study between the signal generated in silicon sensors and the dose delivered in the PMMA (or solid water) phantom, measured with the AM chamber or GafChromic films, will be performed. This could lead to the design of a dose-based beam monitoring approach, e.g., positioning silicon sensors in the edge of the irradiation field and replacing or complementing the beam delivery control based on the sole counting of the number of beam pulses by the PCC.

The characterization of the LINAC beam for different settings reported in this study is preliminary for its future usage in studies of spatial fractionation. Similarly to UHDR irradiations, SFRT demonstrated the ability to spare healthy tissue while maintaining the same effectiveness in controlling tumors, and several research groups are investigating the effects of FLASH and mini-beams both individually and in terms of their potential synergistic actions [16]. The PMMA applicator used in this work, which was demonstrated to increase the dose at the isocenter, could be exploited to hold perforated templates along the beamline and study the dosimetry characteristics of different template configurations (in terms of number, geometry and spacing of holes). The dose peak's full width at half

maximum and peak-to-valley dose ratio could be characterized at the different energies available (from 6 to 18 MeV) and at different dose rates for the 10 MeV electron beam. This could contribute to providing useful information to disentangle the tissue-sparing effects due to UHDR and spatial fractionated beams [15,16]. Finally, the possibility to deliver 18 MeV electron beams will be carefully considered to explore UHDR irradiations at higher energies [27].

5. Conclusions

The LINAC Elekta SL 18 MV has been successfully upgraded to deliver 10 MeV UHDR electron beams. This modification is completely reversible, and switching between the conventional modality and the UHDR modality takes only a few minutes. The LINAC is now capable of reaching a maximum of 2.2 Gy/pulse and an instantaneous dose rate of over 10^5 Gy/s at the crosshair foil position in a pulse lasting 2 μs. A silicon sensor device assesses the stability and repeatability of the pulses across different beam deliveries and days.

In the future, the LINAC could be exploited as a facility for testing beam monitoring and dosimetry devices, as well as for radiobiological experiments to further investigate the FLASH effect. The use of applicators with different geometries and various perforated templates could enable the study of the effects of SFRT and its combination with UHDR irradiation.

References

1. Favaudon, V.; Caplier, L.; Monceau, V.; Pouzoulet, F.; Sayarath, M.; Fouillade, C.; Poupon, M.-F.; Brito, I.; Hupé, P.; Bourhis, J.; et al. Ultrahigh dose-rate FLASH irradiation increases the differential response between normal and tumor tissue in mice. *Sci. Transl. Med.* **2014**, *6*, 245ra93. [CrossRef] [PubMed]
2. Montay-Gruel, P.; Petersson, K.; Jaccard, M.; Boivin, G.; Germond, J.F.; Petit, B.; Doenlen, R.; Favaudon, V.; Bochud, F.; Bailat, C.; et al. Irradiation in a Flash: Unique Sparing of Memory in Mice after Whole Brain Irradiation with Dose Rates above 100 Gy/s. *Radiother. Oncol.* **2017**, *124*, 365–369. [CrossRef] [PubMed]

3. Vozenin, M.C.; De Fornel, P.; Petersson, K.; Favaudon, V.; Jaccard, M.; Germond, J.F.; Petit, B.; Burki, M.; Ferrand, G.; Patin, D.; et al. The Advantage of FLASH Radiotherapy Confirmed in Mini-pig and Cat-cancer Patients. *Clin. Cancer Res.* **2019**, *25*, 35–42. [CrossRef] [PubMed]

4. Hageman, E.; Che, P.-P.; Dahele, M.; Slotman, B.J.; Sminia, P. Radiobiological Aspects of FLASH Radiotherapy. *Biomolecules* **2022**, *12*, 1376. [CrossRef]

5. Di Martino, F.; Barca, P.; Barone, S.; Bortoli, E.; Borgheresi, R.; De Stefano, S.; Di Francesco, M.; Faillace, L.; Giuliano, L.; Grasso, L.; et al. FLASH Radiotherapy With Electrons: Issues Related to the Production, Monitoring, and Dosimetric Characterization of the Beam. *Front. Phys.* **2020**, *8*, 570697. [CrossRef]

6. Romano, F.; Bailat, C.; Jorge, P.G.; Lerch ML, F.; Darafsheh, A. Ultra high dose rate dosimetry: Challenges and opportunities for FLASH radiation therapy. *Med. Phys.* **2022**, *49*, 4912–4932. [CrossRef]

7. Vignati, A.; Giordanengo, S.; Fausti, F.; Martì Villarreal, O.A.; Mas Milian, F.; Mazza, G.; Shakarami, Z.; Cirio, R.; Monaco, V.; Sacchi, R. Beam Monitors for Tomorrow: The Challenges of Electron and Photon FLASH RT. *Front. Phys.* **2020**, *8*, 375. [CrossRef]

8. Giannini, N.; Gadducci, G.; Fuentes, T.; Gonnelli, A.; Di Martino, F.; Puccini, P.; Naso, M.; Pasqualetti, F.; Capaccioli, S.; Paiar, F. Electron FLASH Radiotherapy in Vivo Studies. A Systematic Review. *Front. Oncol.* **2024**, *14*, 1373453. [CrossRef]

9. Rahman, M.; Trigilio, A.; Franciosini, G.; Moeckli, R.; Zhang, R.; Böhlen, T.T. FLASH Radiotherapy Treatment Planning and Models for Electron Beams. *Radiother. Oncol.* **2022**, *175*, 210–221. [CrossRef]

10. Lempart, M.; Blad, B.; Adrian, G.; Bäck, S.; Knöös, T.; Ceberg, C.; Petersson, K. Modifying a Clinical Linear Accelerator for Delivery of Ultra-High Dose Rate Irradiation. *Radiother. Oncol.* **2019**, *139*, 40–45. [CrossRef]

11. Snyder, M.; Vadas, J.; Musselwhite, J.; Halford, R.; Wilson, G.; Stevens, C.; Yan, D. FLASH radiotherapy monitor chamber signal conditioning. *Med. Phys.* **2021**, *48*, 791–795. [CrossRef] [PubMed]

12. Dal Bello, R.; Von Der Grün, J.; Fabiano, S.; Rudolf, T.; Saltybaeva, N.; Stark, L.S.; Ahmed, M.; Bathula, M.; Kucuker Dogan, S.; McNeur, J.; et al. Enabling Ultra-High Dose Rate Electron Beams at a Clinical Linear Accelerator for Isocentric Treatments. *Radiother. Oncol.* **2023**, *187*, 109822. [CrossRef]

13. Cetnar, A.J.; Jain, S.; Gupta, N.; Chakravarti, A. Technical note: Commissioning of a linear accelerator producing ultra-high dose rate electrons. *Med. Phys.* **2024**, *51*, 1415–1420. [CrossRef] [PubMed]

14. Schüler, E.; Trovati, S.; King, G.; Lartey, F.; Rafat, M.; Villegas, M.; Praxel, A.J.; Loo, B.W.; Maxim, P.G. Experimental Platform for Ultra-High Dose Rate FLASH Irradiation of Small Animals Using a Clinical Linear Accelerator. *Int. J. Radiat. Oncol. Biol. Phys.* **2017**, *97*, 195–203. [CrossRef] [PubMed]

15. Yan, W.; Khan, M.K.; Wu, X.; Simone CB 2nd Fan, J.; Gressen, E.; Zhang, X.; Limoli, C.L.; Bahig, H.; Tubin, S.; Mourad, W.F. Spatially fractionated radiation therapy: History, present and the future. *Clin. Transl. Radiat. Oncol.* **2019**, *20*, 30–38. [CrossRef] [PubMed] [PubMed Central]

16. Pensavalle, J.H.; Romano, F.; Celentano, M.; Sarto, D.D.; Felici, G.; Franciosini, G.; Masturzo, L.; Milluzzo, G.; Patera, V.; Prezado, Y.; et al. Realization and dosimetric characterization of a mini-beam/flash electron beam. *Front. Phys.* **2023**, *11*, 1269495. [CrossRef]

17. Medina, E.; Ferro, A.; Abujami, M.; Camperi, A.; Centis Vignali, M.; Data, E.; Del Sarto, D.; Deut, U.; Di Martino, F.; Fadavi Mazinani, M.; et al. First experimental validation of silicon-based sensors for monitoring ultra-high dose rate electron beams. *Front. Phys.* **2024**, *12*, 1258832. [CrossRef]

18. International Atomic Energy Agency. *Absorbed Dose Determination in External Beam Radiotherapy*; Technical Reports Series; Rev. 1; International Atomic Energy Agency: Vienna, Austria, 2024; ISBN 978-92-0-146022-6.

19. Subiel, A.; Moskvin, V.; Welsh, G.H.; Cipiccia, S.; Reboredo, D.; DesRosiers, C.; Jaroszynski, D.A. Challenges of Dosimetry of Ultra-Short Pulsed Very High Energy Electron Beams. *Phys. Medica* **2017**, *42*, 327–331. [CrossRef]

20. McManus, M.; Romano, F.; Lee, N.D.; Farabolini, W.; Gilardi, A.; Royle, G.; Palmans, H.; Subiel, A. The challenge of ionisation chamber dosimetry in ultra-short pulsed high dose-rate Very High Energy Electron beams. *Sci. Rep.* **2020**, *10*, 9089. [CrossRef]

21. Niroomand-Rad, A.; Blackwell, C.R.; Coursey, B.M.; Gall, K.P.; Galvin, J.M.; McLaughlin, W.L.; Meigooni, A.S.; Nath, R.; Rodgers, J.E.; Soares, C.G. Radiochromic film dosimetry: Recommendations of AAPM Radiation Therapy Committee Task Group 55. *Med. Phys.* **1998**, *25*, 2093–2115. [CrossRef]

22. Devic, S.; Seuntjens, J.; Sham, E.; Podgorsak, E.B.; Schmidtlein, C.R.; Kirov, A.S.; Soares, C.G. Precise radiochromic film dosimetry using a flat-bed document scanner. *Med. Phys.* **2005**, *32*, 2245–2253. [CrossRef]

23. Costa, F.; Sarmento, S.; Sousa, O. Assessment of clinically relevant dose distributions in pelvic IOERT using Gafchromic EBT3 films. *Phys. Medica* **2015**, *31*, 692–701. [CrossRef] [PubMed]

24. Strydom, W.; Parker, W.; Olivares, M. Chapter 8 electron beams: Physicaland clinical aspects. In *Radiation Oncology Physics: A Handbook for Teachers and Students*; McGill University: Montreal, QC, Canada; IAEA: Vienna, Austria, 2006; pp. 1–46.

25. Ashraf, M.R.; Rahman, M.; Zhang, R.; Williams, B.B.; Gladstone, D.J.; Pogue, B.W.; Bruza, P. Dosimetry for FLASH Radiotherapy: A Review of Tools and the Role of Radioluminescence and Cherenkov Emission. *Front. Phys.* **2020**, *8*, 328. [CrossRef]

26.   Konradsson, E.; Wahlqvist, P.; Thoft, A.; Blad, B.; Bäck, S.; Ceberg, C.; Petersson, K. Beam control system and output fine-tuning for safe and precise delivery of FLASH radiotherapy at a clinical linear accelerator. *Front. Oncol.* **2024**, *14*, 1342488. [CrossRef] [PubMed]

27.   Faillace, L.; Alesini, D.; Bisogni, G.; Bosco, F.; Carillo, M.; Cirrone, P.; Cuttone, G.; De Arcangelis, D.; De Gregorio, A.; Di Martino, F.; et al. Perspectives in linear accelerator for FLASH VHEE: Study of a compact C-band system. *Phys. Medica* **2022**, *104*, 149–159. [CrossRef]